Tubular and Rodlike Ordered Mesoporous Silicon (Oxy)carbide Ceramics and their Structural Transformations

Piotr Krawiec,*,† Christian Schrage,‡ Emanuel Kockrick,‡ and Stefan Kaskel‡

Instituto de Tecnología Química, UPV-CSIC, Avenida de los Naranjos s/n, 46022 Valencia, Spain, and Institute of Inorganic Chemistry, Dresden University of Technology, Mommsenstrasse 6, D-01062 Dresden, Germany

Received April 15, 2008. Revised Manuscript Received June 5, 2008

Ordered mesoporous silicon carbide ceramics with hexagonal *p6mm* (OM-SiC-3, OM-SiC-5), cubic *Ia3d* (OM-SiC-8) and cubic $I4_1/a$ or lower (OM-SiC-8) pore arrangement symmetries were prepared via nanocasting of SBA-15 and KIT-6 ordered mesoporous silica templates with polycarbosilane (PCS) precursor (numbering of the OM-SiC materials corresponds to their CMK ordered mesoporous carbon analogues). Four different PCS were used for the OM-SiC preparation (liquid SMP-10, low-molecular-weight PCS with $M_W = 800$ melted at 320 °C and PCS with $M_W = 800$, 1400, 3500 dissolved in heptane/butanol). Infiltration of liquid vinyl functionalized SMP-10 precursor, and subsequent pyrolysis in vacuum resulted in OM-SiC-5 materials with tubular structure similar to that of the CMK-5 carbons (according to the TEM, low angle X-ray diffraction and nitrogen physisorption measurements). No significant differences were observed between the direct melt (PCS-800 at 320 °C) and wet impregnation procedure (PCS-800 in heptane/butanol) for OM-SiC-3, whereas significant differences were measured for materials prepared using different molecular weights of the PCS precursors. The influence of different precursor loadings and final pyrolysis temperature was also investigated. In the case of materials prepared from cubic KIT-6, transformation of the OM-SiC-8 symmetry could be observed by small-angle X-ray diffraction.

1. Introduction

Nanocasting is a highly versatile and promising technique for the preparation of ordered mesoporous materials.[1–5] Typically, mesoporous silica and carbons are used as hard templates (exotemplates) not only to prepare three-dimensional structures[6–10] but also for the space confined synthesis of nanowires and nanoparticles.[10–16] Quite a number of reports address the preparation of ordered mesoporous oxides, carbons, and metals using nanocasting;[6–8,17–22] however, only recently was the synthesis of mesoporous or nanostructured carbides and nitrides reported.[2,23–31] Carbide and nitride materials offer extreme temperature resistance[29–32] and have applications in catalysis,[32–36] and thus the preparation of

* Corresponding author. Tel.: 34963877000 (int.78513). Fax: 34963877809. E-mail: pkrawiec@itq.upv.es.
† UPV-CSIC.
‡ Dresden University of Technology.

(1) Yang, H. F.; Zhao, D. Y. *J. Mater. Chem.* **2005**, *15*, 1217.
(2) Valdes-Solis, T.; Fuertes, A. B. *Mater. Res. Bull.* **2006**, *41*, 2187.
(3) Lu, A. H.; Schüth, F. *Adv. Mater.* **2006**, *18*, 1793.
(4) Schüth, F. *Angew. Chem., Int. Ed.* **2003**, *42*, 3604.
(5) Schüth, F. *Chem. Mater.* **2001**, *13*, 3184.
(6) Ryoo, R.; Joo, S. H.; Jun, S. *J. Phys. Chem. B* **1999**, *103*, 7743.
(7) Lu, A. H.; Schmidt, W.; Taguchi, A.; Spliethoff, B.; Tesche, B.; Schüth, F. *Angew. Chem., Int. Ed.* **2002**, *41*, 3489.
(8) Ryoo, R.; Joo, S. H.; Kruk, M.; Jaroniec, M. *Adv. Mater.* **2001**, *13*, 677.
(9) Kang, M.; Yi, S. H.; Lee, H. I.; Yie, J. E.; Kim, J. M. *Chem. Commun.* **2002**, 1944.
(10) Joo, S. H.; Choi, S. J.; Oh, I.; Kwak, J.; Liu, Z.; Terasaki, O.; Ryoo, R. *Nature* **2001**, *412*, 169.
(11) Liu, Z.; Sakamoto, Y.; Ohsuna, T.; Hiraga, K.; Terasaki, O.; Ko, C. H.; Shin, H. J.; Ryoo, R. *Angew. Chem., Int. Ed.* **2000**, *39*, 3107.
(12) Krawiec, P.; Kockrick, E.; Auffermann, G.; Simon, P.; Kaskel, S. *Chem. Mater.* **2006**, *18*, 2663.
(13) Kockrick, E.; Krawiec, P.; Schnelle, W.; Geiger, D.; Schappacher, F. M.; Pottgen, R.; Kaskel, S. *Adv. Mater.* **2007**, *19*, 3021.
(14) Corma, A. *Chem. Rev.* **1997**, *97*, 2373.
(15) Taguchi, A.; Schüth, F. *Microporous Mesoporous Mater.* **2005**, *77*, 1.
(16) Shin, H. J.; Ko, C. H.; Ryoo, R. *J. Mater. Chem.* **2001**, *11*, 260.
(17) Polarz, S.; Antonietti, M. *Chem. Commun.* **2002**, 2593.
(18) Kleitz, F.; Choi, S. H.; Ryoo, R. *Chem. Commun.* **2003**, 2136.
(19) Rumplecker, A.; Kleitz, F.; Salabas, E. L.; Schüth, F. *Chem. Mater.* **2007**, *19*, 485.
(20) Polarz, S.; Orlov, A. V.; Schüth, F.; Lu, A. H. *Chem.—Eur. J.* **2007**, *13*, 592.
(21) Jun, S.; Joo, S. H.; Ryoo, R.; Kruk, M.; Jaroniec, M.; Liu, Z.; Ohsuna, T.; Terasaki, O. *J. Am. Chem. Soc.* **2000**, *122*, 10712.
(22) Yang, C. M.; Weidenthaler, C.; Spliethoff, B.; Mayanna, M.; Schuth, F. *Chem. Mater.* **2005**, *17*, 355.
(23) Dibandjo, P.; Bois, L.; Chassagneux, F.; Cornu, D.; Letoffe, J. M.; Toury, B.; Babonneau, F.; Miele, P. *Adv. Mater.* **2005**, *17*, 571.
(24) Dibandjo, P.; Bois, L.; Chassagneux, F.; Miele, P. *J. Eur. Ceram. Soc.* **2007**, *27*, 313.
(25) Yant, J.; Wang, A. J.; Kim, D. P. *J. Phys. Chem. B* **2006**, *110*, 5429.
(26) Yoon, T. H.; Lee, H. J.; Yan, J.; Kim, D. P. *J. Ceram. Soc. Jpn.* **2006**, *114*, 473.
(27) Krawiec, P.; Geiger, D.; Kaskel, S. *Chem. Commun.* **2006**, *23*, 2469.
(28) Krawiec, P.; Weidenthaler, C.; Kaskel, S. *Chem. Mater.* **2004**, *16*, 2869.
(29) Shi, Y. F.; Meng, Y.; Chen, D. H.; Cheng, S. J.; Chen, P.; Yang, T. F.; Wan, Y.; Zhao, D. Y. *Adv. Funct. Mater.* **2006**, *16*, 561.
(30) Ledoux, M. J.; Pham-Huu, C. *Cattech* **2001**, *5*, 226.
(31) Krawiec, P.; Kaskel, S. *J. Solid State Chem.* **2006**, *179*, 2281.
(32) Sung, I. K.; Christian; Mitchell, M.; Kim, D. P.; Kenis, P. J. A. *Adv. Funct. Mater.* **2005**, *15*, 1336.
(33) Ramanathan, S.; Oyama, S. T. *J. Phys. Chem.* **1995**, *99*, 16365.
(34) Rodrigues, J. A. J.; Cruz, G. M.; Bugli, G.; Boudart, M.; DjegaMariadassou, G. *Catal. Lett.* **1997**, *45*, 1.
(35) Krawiec, P.; De Cola, P. L.; Gläser, R.; Weitkamp, J.; Weidenthaler, C.; Kaskel, S. *Adv. Mater.* **2006**, *18*, 505.
(36) Corma, A.; Huber, G. W.; Sauvanaud, L.; O'Connor, P. *J. Catal.* **2007**, *247*, 307.

10.1021/cm801035g CCC: $40.75
Published on Web 08/02/2008

nanostructured mesoporous or nanoparticulate silicon carbide, silicon carbonitride, and silicon oxycarbide was discussed.[27–29,31,37–51] Silicon carbide is an inert semiconductor material with high hardness, high temperature stability, and excellent heat conductivity.[30,31] Therefore, SiC is an important catalyst support for highly exothermic reactions at high temperatures. Nanostructured SiC can be used as a bulk material or as a key component of nanocomposites causing increased plasticity and enhanced tribological performance.[52–54]

Hard templates such as ordered mesoporous silica were recently used for the preparation of high surface area mesoporous silicon carbide. Reaction of the carbon source with silica (Acheson process) was applied using MCM and SBA type materials filled with a carbon precursor (or inverse) at high temperatures.[40–47] However, the silicon carbide formation directly from silica and carbon requires high temperatures and in the first step proceeds via gaseous intermediates (SiO and CO), causing a collapse of the ordered mesoporous structure and lower specific surface areas (up to 260 $m^2\ g^{-1}$).[42,46] This process was recently studied and described in more details by Wang et al. and Yao et al., who also showed that only disordered (on the mesoscale) materials can be obtained via this method.[45,47] The main advantage of this carbothermal process is the high crystallinity of the SiC materials. One can also expect lower oxygen content for carbothermal procedure because of carbon excess as well as the lower specific surface areas (lower amount of the surface oxycarbide species). On the other hand, Yu el.al showed how the carbothermal reduction can be used for the in situ preparation of the titanium carbide nanoparticles inside the walls of ordered mesoporous carbons. Direct deposition of silicon carbide in a silica matrix via CVD process and subsequent dissolving of silica in HF produces poorly ordered mesoporous SiC.[28,31]

Infiltration of mesoporous oxides with polycarbosilanes (PCS) and their subsequent transformation to SiC at 1200 to 1400 °C produces well-ordered materials with high surface areas up to 800 $m^2\ g^{-1}$ (Scheme 1A).[27,29] Two methods for the polycarbosilane infiltration were developed by Shi et.al. (high-molecular-weight PCS dissolved in organic solvent)[29] and Krawiec et al. (melted low-molecular-weight PCS without solvent).[27] Using the same approach and ordered mesoporous carbon (CMK-3) as template, Shi et al. prepared ordered mesoporous silicon oxycarbide and carbonitride in a pyrolysis under oxygen (silicon oxycarbide) or ammonia (silicon carbonitride) atmosphere.[55] During the pyrolysis step, the CMK-3 template was removed by either oxygen or ammonia leaving the ordered mesoporous inverse replica.

Scheme 1. Synthesis Routes for the Preparation of Ordered Mesoporous Silicon Carbides with Hexagonal Ordering of Mesopores and Rodlike (A, OM-SiC-3) or Tubular (B, OM-SiC-5) Structure; P1 are the Pores between Rods/Tubes, While in the Case of the Tubular OM-SiC-5, Additional P2 Pores Can Be Detected in the Interior Part of the Tubes

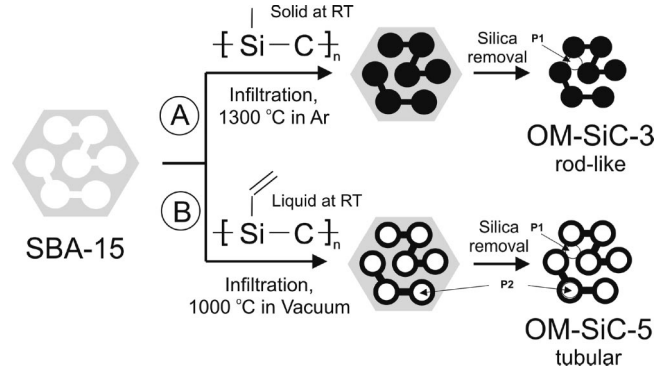

Here, we report for the first time preparation of tubular SiC inverse replica of mesoporous silica (SBA-15). This was achieved by using liquid vinyl functionalized polycarbosilane precursor of SiC and its high temperature treatment under a vacuum. Resulting material is composed of hexagonally ordered nanopipes and has bimodal pore size distribution (pores between the tubes and in the tubes (CMK-5-like, Scheme 1B). A tubular inverse replica was reported only for the carbon materials until now (CMK-5).[10,56–60] Moreover, we also analyzed different infiltration conditions of SBA-15 and structural transformation of the SiC inverse replica of the cubic KIT-6 using low-angle XRD.

2. Experimental Section

OM-SiC-3 and OM-SiC-8 Synthesis. In a typical synthesis procedure, 1.5 g of the SBA-15 or KIT-6 (prepapred according to ref [18,61]) was infiltrated with the appropriate amount of polycarbosilane precursor (PCS precursors with different molecular weights were obtained from Aldrich). The quantity of PCS was calculated from the A parameter in Tables 1 and 3 knowing the total pore volume of silica template (Supporting Information Table S1).

(37) Gupta, P.; Wang, W.; Fan, L. S. *Ind. Eng. Chem. Res.* **2004**, *43*, 4732.
(38) Guo, X. Y.; Jin, G. Q. *J. Mater. Sci.* **2005**, *40*, 1301.
(39) Pol, V. G.; Pol, S. V.; Gedanken, A. *Chem. Mater.* **2005**, *17*, 1797.
(40) Parmentier, J.; Patarin, J.; Dentzer, J.; Vix-Guterl, C. *Ceram. Int.* **2002**, *28*, 1.
(41) Liu, Z. C.; Shen, W. H.; Bu, W. B.; Chen, H. R.; Hua, Z. L.; Zhang, L. X.; Li, L.; Shi, J. L.; Tan, S. H. *Microporous Mesoporous Mater.* **2005**, *82*, 137.
(42) Lu, A. H.; Schmidt, W.; Kiefer, W.; Schüth, F. *J. Mater. Sci.* **2005**, *40*, 5091.
(43) Yang, Z. X.; Xia, Y. D.; Mokaya, R. *Chem. Mater.* **2004**, *16*, 3877.
(44) Vix-Guterl, C.; Alix, I.; Gibot, P.; Ehrburger, P. *Appl. Surf. Sci.* **2003**, *210*, 329.
(45) Yao, J. F.; Wang, H. T.; Zhang, X. Y.; Zhu, W.; Wei, J. P.; Cheng, Y. B. *J. Phys. Chem. C* **2007**, *111*, 636.
(46) Sonnenburg, K.; Adelhelm, P.; Antonietti, M.; Smarsly, B.; Noske, R.; Strauch, P. *Phys. Chem. Chem. Phys.* **2006**, *8*, 3561.
(47) Wang, K.; Yao, J. F.; Wang, H. T.; Cheng, Y. B. *Nanotechnology* **2008**, *19*, 175605.
(48) Nghiem, Q. D.; Kim, D.; Kim, D. P. *Adv. Mater.* **2007**, *19*, 2351.
(49) Kockrick, E.; Krawiec, P.; Petasch, U.; Martin, H. P.; Herrmann, M.; Kaskel, S. *Chem. Mater.* **2008**, *20*, 77.
(50) Kamperman, M.; Du, P.; Scarlat, R. O.; Herz, E.; Werner-Zwanziger, U.; Graf, R.; Zwanziger, J. W.; Spiess, H. W.; Wiesner, U. *Macromol. Chem. Phys.* **2007**, *208*, 2096.
(51) Malenfant, P. R. L.; Wan, J. L.; Taylor, S. T.; Manoharan, M. *Nat. Nanotechnol.* **2007**, *2*, 43.
(52) Mitomo, M.; Kim, Y. W.; Hirotsuru, H. *J. Mater. Res.* **1996**, *11*, 1601.
(53) Groza, J. R. *Int. J. Powder Metall.* **1999**, *35*, 59.
(54) Groza, J. R. *Nanostruct. Mater.* **1999**, *12*, 987.
(55) Shi, Y. F.; Wan, Y.; Zhai, Y. P.; Liu, R. L.; Meng, Y.; Tu, B.; Zhao, D. Y. *Chem. Mater.* **2007**, *19*, 1761.
(56) Kruk, M.; Jaroniec, M.; Kim, T. W.; Ryoo, R. *Chem. Mater.* **2003**, *15*, 2815.
(57) Che, S. N.; Lund, K.; Tatsumi, T.; Iijima, S.; Joo, S. H.; Ryoo, R.; Terasaki, O. *Angew. Chem., Int. Ed.* **2003**, *42*, 2182.
(58) Lu, A. H.; Li, W. C.; Schmidt, W.; Kiefer, W.; Schüth, F. *Carbon* **2004**, *42*, 2939.
(59) Solovyov, L. A.; Kim, T. W.; Kleitz, F.; Terasaki, O.; Ryoo, R. *Chem. Mater.* **2004**, *16*, 2274.
(60) Lu, A. H.; Schmidt, W.; Spliethoff, B.; Schüth, F. *Adv. Mater.* **2003**, *15*, 1602.
(61) Choi, M.; Heo, W.; Kleitz, F.; Ryoo, R. *Chem. Commun.* **2003**, 1340.

Table 1. OM-SiC-3 Materials Pyrolyzed at 1300 °C from Aldrich PCS

sample code[a]	T_{silica} (°C)[b]	PCS [c]	A (g cm^{-3})[d]	S_g^{comp} (m^{2}g^{-1})[e]	V_p (cm^{3}g^{-1})[f]	S_g^{SiC} (m^{2}g^{-1})[g]
SiC-3-M08-135	135	800 M	0.89	61	0.56	667
SiC-3-S08-135	135	800 S	0.89	59	0.58	685
SiC-3-S14-135	135	1400 S	0.89	77	0.68	672
SiC-3-S35-135	135	3500 S	0.89	54	0.52	449
SiC-3-M08-130	130	800 M	0.91	90	0.48	648
SiC-3-S14-130	130	1400 S	0.91	65	0.58	634
SiC-3-S08-80A	80	800 S	1.40	5	0.57	899
SiC-3-S08−80B	80	800 S	1.14	7	0.63	940
SiC-3-S08-80C	80	800 S	0.92	5	0.62	929
SiC-3-S08-80D[h]	80	800 S	0.75	7	[h]	[h]
SiC-3-S08-50[h]	50	800 S	0.90	6	[h]	[h]

[a] Sample codes are SiC-3-ZXX-YYY, where Z is infiltration method (M, melt at 320 °C; S, solution infiltration using the heptane/BuOH as solvent), XX is PCS precursor code, 08 is PCS with M_w = 800; 14 and 35 is PCS with M_w = 1400 and 3500. Suffixes A, B, C, D are used to differentiate samples prepared with different PCS amounts. [b] Temperature of hydrothermal treatment of SBA-15 silica [c] Polycarbosilane molecular weight and method of infiltration: M is melt infiltration at 320 °C, S is wet infiltration using heptane/BuOH as solvent. [d] Mass of PCS used for infiltration of 1 cm^3 of the pore volume of silica. [e] Specific surface area of SiC/SBA-15 composite before HF treatment. [f] Pore volume of SiC. [g] Specific surface area of SiC. [h] Less than 22% ceramic yield after HF treatment and filtration; most of the sample remained in the filtrate.

Table 2. OM-SiC-5 Materials Prepared from Starfire SMP-10 Liquid Polycarbosilane; All Samples (except SiC-5-135-VM and SiC-5-135 prepared in vacuum at 1000 °C) were Pyrolyzed in Argon at 1300 °C[c]

sample code[a]	T_{silica} (°C)	T_{Inf} (°C)[b]	A (g/cm^3)[c]	S_g^{comp} (m^{2}g^{-1})[d]	V_p (cm^{3}g^{-1})[e]	S_g^{SiC} (m^{2}g^{-1})[f]
SiC-5-130-90X	130	90	0.91	15	0.52	648
SiC-5-130-250	130	250	0.91	14	0.68	800
SiC-5-130-250A	130	250	0.76	86	0.57	710
SiC-5-130-350	130	350	0.76	70	0.51	639
SiC-5-135-VM	135	250−450[g]	0.91	309	0.82	926
SiC-5-135-VL	135	150[h]	0.91	197	0.76	840

[a] Sample codes are SiC-5-YYY-ZZZ, where YYY is the temperature of silica hydrothermal treatment and ZZZ is typically the temperature of polycarbosilane infiltration in °C. Suffix X is means infiltration in air, whereas suffix A is sample prepared with lower PCS ammount than the sample above in the table, VM is vacuum-treated sample prepared by melt-impregnation, VL is vacuum treated sample prepared by solvent infiltration. [b] Temperature of SMP-10 infiltration. [c] Mass of PCS used for infiltration of 1 cm^3 of the pore volume of silica. [d] Specific surface area of SiC/SBA-15 composite before HF treatment. [e] Pore volume of SiC. [f] Specific surface area of SiC. [g] Infiltration at 250 °C in argon was carried for 12 h, changed to vacuum, heated to 450 °C (50 °C h^{1-}), and left under constant evacuation for 12 h. [h] Infiltration at 150 °C in argon from SMP-10/heptane solution, followed by drying in argon/vacuum at the same temperature.

In the case of melt impregnation, the SBA-15 template was placed in the Schlenk tube, degassed at 250 °C under a vacuum, and subsequently flooded with argon. To this was added polycarbosilane precursor, which was then mixed and heated to 320 °C. At this point, the sample was agitated for 1 h (under flowing argon) and then kept in the closed tube for 12 h.

In the case of wet impregnation with organic solvents, typically a solution of appropriate amount of PCS in a mixture of heptane/BuOH (50/0.3 mL) was used for the impregnation of 1.5 g of SBA-15. The mixture was then left overnight for evaporation in a hood in an opened beaker, under constant stirring.

The PCS infiltrated SBA-15 and KIT-6 silicas were placed in an alumina boat and in a tubular furnace under constant argon flow (40 mL min^{-1}) and heat treatment was conducted according to the following temperature program:[29] RT−300 °C at 150 °C h^{-1}, then 5 h at 300 °C, followed by heating to 700 °C at 30 °C h^{-1}. After reaching 700 °C, the sample was heated to desired pyrolysis temperature at 120 °C h^{-1} and maintained for 2 h. However, we conducted experiments that showed no significant changes in properties of OM-SiC-3 materials if a simple heating ramp of 50 °C h^{-1} was used directly from RT to reach the desired pyrolysis temperature.[27]

As-obtained OM-SiC-3/Silica and OM-SiC-8/Silica composites samples were dissolved in a mixture of EtOH/H_2O/40% HF (each one 40 mL), shaken and left for 1 h for silica etching. The solution was then filtered over a filter paper and washed with large amounts of EtOH (∼200 mL). The OM-SiC materials were left for overnight drying in a hood (in the same filter) and collected next day.

The ceramic yield was calculated by comparing the mass of dried OM-SiC product collected from the filter paper and the mass of polycarbosilane precursor used for infiltration. For the pure PCS precursor with molecular weight of 800 (pyrolyzed without silica template), a low ceramic yield of ∼60 wt % was observed, because of the partial evaporation of the precursor. The increase in the molecular weight to 3500 resulted in higher ceramic yield of ∼70 wt %. However, the ceramic yield depends on exact pyrolysis conditions and chemical composition. More details on polycarbosilane precursors and their expected ceramic yields can be found in the literature.[62,63]

Tubular OM-SiC-5 Synthesis. In a typical synthesis procedure, 1.5 g of the SBA-15 was infiltrated with the appropriate amount of polycarbosilane precursor (vilnyl functionalized SMP-10 precursor was obtained from Starfire). The quantity of SMP-10 was calculated from the A parameter in Table 2 knowing the total pore volume of silica template (Supporting Information Table S1). SBA-15 template was placed in the Schlenk tube, degassed at 250 °C under vacuum and subsequently flooded with argon. To this was added polycarbosilane SMP-10 precursor, and the solution was mixed and heated to the desired infiltration temperature (Table 2, T_{inf}). As an exception, the SiC-5-130-90X sample was infiltrated in an air atmosphere. In the case of SiC-5-135-VM, the mixed argon/vacuum infiltration was used. For this sample, in the first step, SMP-10 was infiltrated in argon at 250 °C (1 h agitation, then 12 h static atmosphere in closed tube) and subsequently agitated for 10 min and heated under a vacuum in the same tube to 450 °C (heating ramp 50 °C h^{-1}); it remained under constant evacuation for another 12 h. A similar procedure was applied in case of SiC-5-135VL, but the SMP-10 precursor was mixed with heptane (1:3 weight ratio) prior to the infiltration, and the organic solvent was removed at 150 °C for 5 h.

(62) Laine, R. M.; Babonneau, F. *Chem. Mater.* **1993**, *5*, 260.
(63) Interrante, L. V.; Shen, Q. Polycarbosilanes. In *Silicon-Containing Polymers*; Kluwer Academic: Dordrecht, The Netherlands, 2000 244.

For pyrolysis (final heat treatment), infiltrated SMP-10/silica materials were collected and treated in an argon atmosphere in an alumina boat in tubular furnace (40 mL min^{-1} Ar flow), or in a vacuum in a quartz tube under constant evacuation. The samples were then heated to the desired temperature with a heating ramp of 50 °C $h^{-1,}$ and remained at that temperature for 2 h. In all experiments, the furnace was cooled by switching off without any controlled ramp.

The obtained OM-SiC-5/silica composites were treated with HF solution in the same manner as OM-SiC-3/silica materials in order to remove silica. The ceramic yield was calculated in the same manner as the for the OM-SiC-3 materials. The ceramic yield of the pure SMP-10 precursor (without silica template) can be up to 80 wt % (when using the appriopriate conditions), which is considered a high value among the SiC precursors.[62] In the case of the heating ramps applied here, the ceramic yield of the pure SMP-10 was lower (50−55 wt %)

Analysis. Small angle X-ray diffraction patterns were measured on the Nanostar (Bruker), using Cu *K*α radiation and HiStar 2D detector.

The nitrogen physisorption isotherms were measured at −196 °C using a Quantachrome Autosorb 1C apparatus. Prior to the measurement, the samples were evacuated at 150 °C for 5 h. Specific surface areas were calculated using the BET equation in a relative pressure range between $P/P_o = 0.05-0.2$. The pore size distribution was estimated from the adsorption branch of the isotherm using the BJH method assuming a cylindrical pore model. The pore wall thickness of KIT-6 presented in the Supporting Information was calculated according to Ravikovitch for the cubic *Ia3d* silica et al.[64,65]

Elemental analysis were performed using high-temperature combustion (carbon: C200 analyzer from LECO) and hot gas extraction method (oxygen, hydrogen: TCH600 from LECO). Standard SiC materials were used to confirm the quality of the carbon elemental analysis; for them, 30 wt % C was detected with ±0.4 wt % deviation.

3. Results and Discussion

Experiments were divided into four parts. First the influence of preparation methods and conditions on the final structure of the rod-like ordered hexagonal OM-SiC-3 was investigated. For this part, a comparison between melt and wet impregnation of PCS with different molecular weights was made. In the second part, the preparation of the tubular hexagonal replica OM-SiC-5 is discussed, using the liquid PCS precursor containing vinyl groups. In the third part, the influence of the pyrolysis temperature (800−1300 °C) on the specific surface area and chemical composition is presented. The last part shows symmetry transformations of the cubic OM-SiC-8 materials prepared from the cubic KIT-6 ordered mesoporous silica hydrothermally treated at various temperatures.

3.1. Influence of Preparation Conditions and Different Silica Templates on the Properties of Hexagonally Ordered OM-SiC-3 Materials with Nanorod Structure. Eleven OM-SiC-3 samples were prepared (Scheme 1A) using SBA-15 templates (Table 1). Four different SBA-15 templates, hydrothermally treated at 135, 130, 80, and 50 °C, were used and two methods of PCS infiltration into the mesopore system were employed. Such choice of hydrothermal treatment temperatures gives silicas with pore sizes between 4.5 and 11 nm (for 50 and 135 °C, respectively; see the Supporting Information, Table S1). The 80 °C hydrothermal treatment is considered in the literature as the minimal temperature required for the formation of interconnectivity between mesopores in SBA-15 (necessary for the preparation of the inverse replica).[66] One method to introduce PCS into the mesopores of silica is wet impregnation, where SBA-15 powder is added to a solution of PCS in heptane/butanol, and the organic solvent is evaporated overnight.[29] The second method is melt impregnation, where melted low-molecular-weight PCS is infiltrated under argon at 320 °C into SBA-15 (without solvent) and PCS is forced into the mesopore system of silica via capillary forces.[27] For each sample an *A* parameter is given, which defines the specific amount of PCS precursor used per one cm^3 of the mesopore volume of silica template. Three different PCS precursors with various molecular weights (800, 1400, and 3200) were used for wet infiltration, whereas for the melt impregnation, only low-molecular-weight precursor was used ($M_w = 800$). All materials were prepared using the same heating ramp with a final treatment at 1300 °C.

Low- and High-Angle XRD. Low angle X-ray diffraction patterns confirmed that the ordered SiC rod-like inverse replica of SBA-15 was obtained for almost all materials (except SiC-S08-50 and SiC-S08-80D). The reason for the disordered structure of the SiC-S08-50 sample was the lack of the connectivity between the mesopores of silica template synthesized at low temperature (50 °C)[66] and subsequent collapse of the nanorod network, after removal of silica. For the same sample, filtration that was performed after HF treatment (silica removal) resulted in only a low ceramic yield of 22 wt %. The typical ceramic yield from the other samples that had ordered structure was between 70 and 77 wt %. This is significantly higher than for the pyrolysis of the low-molecular-weight PCS precursor alone and can be explained in terms of capillary condensation effect of liquid precursor in pores (which prevents it from being evaporated before cross-linking) and as being due to the formation of silicon oxycarbide species. The same effect was also observed for the second disordered sample (SiC-S08-80D, 15 wt % of ceramic yield), which on the other hand, was produced using a template with interconnected mesopores, but the amount of infiltrated PCS precursor used was too low to form a stable inverse replica ($A = 0.75$). In both cases, the filtrate had black color, suggesting that the disordered particles easily passed the filter resulting in low yields. When the amount of PCS was increased ($A = 0.92$), the replica became stable and a reflection confirming the ordering of mesopores could be observed (SiC-3-S80-80C, Figure 1). A peak at the same position ($2\theta = 1.34$ °) could also be observed for the other materials prepared using the 80 °C template and even larger amounts of PCS ($A = 1.14$ and 1.40, samples SiC-3-S08-80B and SiC-3-S08-80A, respectively). By comparing the position (100) reflection of silica, the unit cell was shrinked by 28.3%. This can be attributed to the lower density of the silica walls in template hydro-

(64) Ravikovitch, P. I.; Neimark, A. V. *Langmuir* **2000**, *16*, 2419.
(65) Sun, J. H.; Coppens, M. O. *J. Mater. Chem.* **2002**, *12*, 3016.
(66) Galarneau, A.; Cambon, N.; Di Renzo, F.; Ryoo, R.; Choi, M.; Fajula, F. *New J. Chem.* **2003**, *27*, 73.

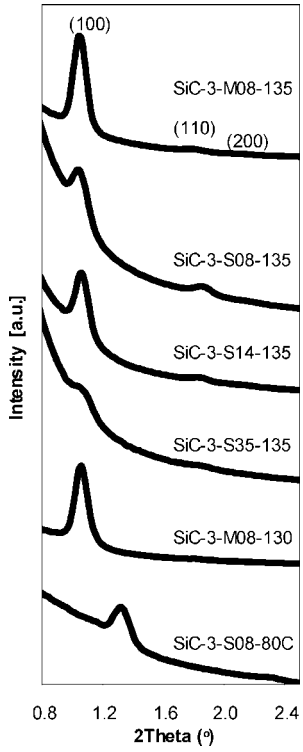

Figure 1. Low-angle XRD patters of OM-SiC-3 materials prepared at 1300 °C.

thermally treated at 80 °C, which results in severe schrinkage at 1300 °C, where silica densifies rapidly.

An SBA-15 template prepared at 135 °C was used to compare the influence of different infiltration methods (melt impregnation and wet infiltration) and various molecular weights of precursors (800, 1400, 3500) on the ordering of OM-SiC-3 materials. For the sample prepared via melt impregnation (SiC-3-M08,135, Figure 1), a clear reflection at 1.06 °2θ could be observed that can be assigned to the (100) plane of the hexagonal *p6mm* mesopore arrangement. The calculated shrinkage of mesostructure (18.8%) is significantly lower as compared to the 80 °C template.[27,29] The other reflections (110) and (200) were very small. On the other hand, when the same PCS precursor was introduced via the wet impregnation method, the (100) reflection was slightly less intense, the background was higher, and the second visible peak gained slightly on the intensity (SiC-3-S08-135, Figure 1). The increase in the PCS molecular weight to 1400 did not result in significant changes in the diffraction pattern (SiC-3-S14-135, Figure 1). However, when the molecular weight was further increased to 3500, the mesoporous silicon carbide obtained was disordered and only a very broad reflection could be observed in the low angle area (SiC-3-S35,135, Figure 1). This indicates that too large polymer molecules were not able to either enter the mesopores or fill the microporous connection between them.

The experiments with silica templates prepared at 130 °C showed the same tendency. As an example, a SAXS pattern of SiC-3-M08-130 is presented in Figure 1. As in the case of SiC-3-M08-135, the SiC-3-M08-130 sample showed one intense (100) reflection and almost absent (110) and (200) peaks, whereas the material prepared via the wet impregnation, SiC-3-S14-130 (using the same silica template and using higher-molecular-weight PCS) had higher background and a second visible peak.

According to the wide-angle X-ray diffraction patterns (see the Supporting Information, Figure S3), all materials discussed in this paragraph (pyrolyzed at 1300 °C from Aldrich PCS precursors) were composed of nanocrystalline cubic β-SiC, as reported previously.[27] However, the degree of silicon carbide crystallization in each sample was dependent on the silica template that was used for the preparation. Mesoporous silicon carbides prepared from templates hydrothermally treated at lower temperatures (smaller pore diameter) were less crystalline (see the Supporting Information, Figure S3, SiC-3-S08-80). On the other hand, large pores of the high-temperature-treated silica allowed better crystallization (SiC-3-S08-135), similar to that of the bulk SiC prepared without template from the same PCS precursor (bulk SiC). More details of the chemical composition are given in the section 3.3.

These results show that the ordered OM-SiC-3 materials can be prepared from SBA-15 templates synthesized in the temperature range between 80 and 135 °C. As expected, SiC samples prepared from templates obtained at low temperature (50 °C) are disordered because of the lack of the mesopore connectivity in the silica template.[66] Two different PCS infiltration methods (wet impregnation and solvent-free melt impregnation) result in well-ordered materials; however, they have slightly varying background and peak intensity ratios.

Nitrogen Physisorption Measurements. All ordered OM-SiC-3 materials showed type IV nitrogen adsorption isotherms (the disordered samples SiC-3-S-14-80D and SiC-3-S14-50 were not characterized). The measured specific surface area was in the range between 449 and 940 $m^2\ g^{-1}$ and depended strongly on the properties of hard silica template and PCS which was used for the synthesis. The smallest specific surface area (449 $m^2\ g^{-1}$) was measured for the SiC-3-S35-135 sample when the PCS precursor with highest molecular weight (3500) was used. This shows that the high-molecular-weight polymer was not able to enter properly the mesopore and micropore system of the silica template, although the silica material synthesized at 135 °C with the largest mesopores of 11 nm in diameter was used. This is in good agreement with the previously discussed low-angle X-ray diffraction data, which showed very poor mesostructure ordering of this sample. Materials prepared from PCS with lower molecular weights (800, 1400) and templates hydrothermally treated at high temperatures had higher specific surface areas (between 634 and 672 $m^2\ g^{-1}$). However, even higher specific surface areas were measured for ordered samples prepared from 80 °C template (SiC-3-S08-80A,B,C, 890−940 $m^2\ g^{-1}$). The latter is due to the smaller pore diameter of SBA-15 treated at 80 °C (7.3 nm), which results in a decrease in the rod diameter in OM-SiC-3 materials.

OM-SiC-3 samples prepared from low-temperature-treated SBA-15 (SiC-3-S08-80A,B,C) have small pore diameter, in the micropore range (<2 nm) (Figure 2). On the other hand, samples prepared from large pore templates (hydrothermally

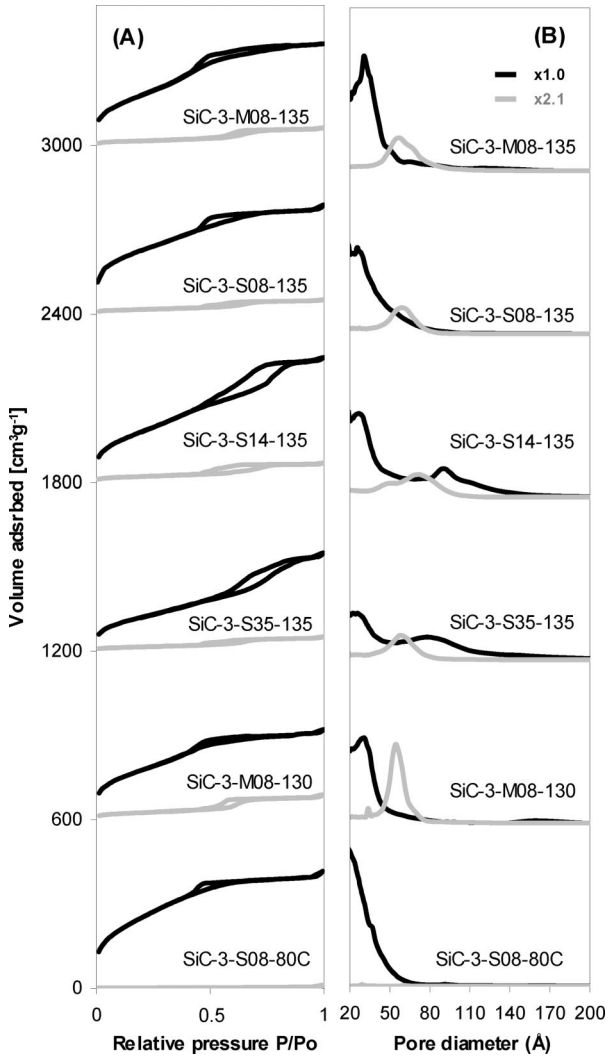

Figure 2. (A) Nitrogen physisorption isotherms (offset 0, 600, 1200, 1800, 2400, 3000 for each following sample from the bottom); (B) BJH pore size distributions (calculated from adsorption branch of isotherm) of OM-SiC-3 materials prepared at 1300 °C. Black lines indicate OM-SiC-3 materials, whereas gray lines represent their composites (before HF treatment).

treated at higher temperatures) show not only larger pore diameters (3 nm) but also often a bimodal pore size distribution (Figure 2). The amount of secondary mesopores in OM-SiC-3 (5−15 nm in diameter) is generally increasing with the increasing molecular weight of the PCS precursor (Figure 2, samples SiC-3-XX-135). Also, the mesopore volume increases when the molecular weight of PCS increases from 800 to 1400. In the case of the SiC-3-S35-135 sample (PCS with $M_w = 3500$), the pore volume is still very high (0.52 $cm^3\ g^{-1}$), although the specific surface area was very low (449 $m^2\ g^{-1}$).

Before the removal of silica with HF, SBA-15/SiC composites prepared from high-temperature-treated silica (130, 135 °C) typically have high specific surface areas between 54 and 90 $m^2\ g^{-1}$, which can be assigned to the incomplete SBA-15 pore filling. The remaining pores have a diameter in the range of 5−7 nm (Figure 2B), which can represent partially filled pores of SBA-15 (after 15−20% shrinkage of the hexagonal mesostructure unit cell at 1300 °C).[27,29] However, after silica removal, this range of pore sizes is not reflected on the pore size distribution of the OM-SiC-3 materials (Figure 2B samples SiC-3-XX-135, 130). Such secondary large mesopore system (5−15 nm) in the OM-SiC-3 samples is probably a result of the incomplete or irregular filled pore structure of the composite, resulting in defects in the network or due to the presence of SiC nanoparticles on the external surface of SBA-15 template. This explanation is also supported by the low angle diffractograms ruling out the nanotube formation which could also lead to a bimodal pore system. The presence of the secondary mesopores in ordered mesoporous silicon carbide was also reported by Shi et al. when large pore cubic silica was used as a template.[29]

In the case of silica templates prepared at 80 °C, by using the same amount of PCS precursor for specific pore volume ($A = 92$, sample SiC-S08-80C), one could fill the mesopore system completely (specific surface area of composites was below 7 $m^2\ g^{-1}$). None of the samples prepared from this template show secondary large mesopores.

Conclusions for the Preparation of OM-SiC-3 Materials. Ordered mesoporous silicon carbide materials with hexagonal pore arrangement (OM-SiC-3) were successfully prepared from SBA-15 templates hydrothermally treated in the temperature range between 80 and 135 °C. OM-SiC-3 materials prepared from 80 °C silica had a higher surface area (up to 940 $m^2\ g^{-1}$) and a pore size in the micropore range (<2 nm), whereas SiC prepared from "135 °C silica" had lower specific surface area (685 $m^2 g^{-1}$) and larger pores (3 nm). No significant differences were observed for materials prepared via melt and wet impregnation of the low molecular weight PCS (similar surface area, pore size distribution, and well-ordered structure). However, the increase in PCS molecular weight resulted in formation of secondary larger mesopores (5−15 nm) and bimodal pore size distributions (and also in a disordered structure for $M_w = 3500$). On the basis of the low-angle X-ray diffraction and pore size distributions of SBA-15/SiC composites and OM-SiC-3 materials, the formation of tubular structures can be ruled out. In our opinion, too high molecular weight and too low amount of PCS precursors can cause the formation of defects in OM-SiC-3 or deposition of nanoparticles outside the pore system causing the bimodal porosity. A bimodal pore size distribution was also observed by Shi. et.al when large pore KIT-6 templates were used and PCS with $M_W = 1500$.[29] The crystallinity of materials decreases when templates with smaller pore sizes are used (see the Supporting Information, Figure S3).

3.2. Preparation of Hexagonally Ordered OM-SiC-5 Materials with Tubular Structure. Tubular, hexagonally ordered OM-SiC-5 materials were prepared using a liquid vinyl functionalized polycarbosilane precursor (SMP-10). Various pyrolysis atmospheres (air, argon, vacuum) and temperatures (1000 and 1300 °C) were studied. As a template, SBA-15 silica materials prepared at 130 and 135 °C were used (with pore diameter of 10 and 11 nm and pore volume of 1.11 and 1.42 $cm^3\ g^{-1}$, respectively). The tendency of SMP-10 precursor to form the thin coating

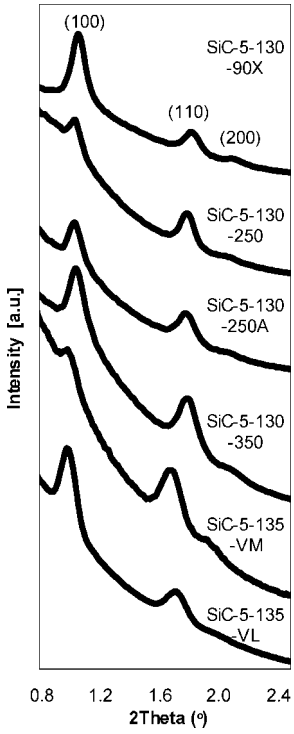

Figure 3. Low-angle X-ray diffraction patterns of the OM-SiC-5 samples pyrolyzed at 1300 °C in argon or at 1000 °C in a vacuum (-VM and -VL materials).

on the surface of pores [Scheme 1B] can be explained in terms of the π-bond (double bond of vinyl group) and silica interactions.[67,68] Such interactions are not present in the PCS precursor used for the preparation of rodlike replica (Scheme 1A), where only methyl terminal groups are present and those do not interact with silica. Moreover, the vacuum treatment and lower molecular weight (liquid state) of SMP-10 are preferential for avoiding the capillary condensation and complete pore filling.

After the SMP-10 infiltration, samples were pyrolyzed in argon at 1300 °C, or in vacuum at 1000 °C (SiC-5-135-VM and SiC-5-135-VL). Except SiC-5-135-VL (prepared via wet impregnation), all samples were prepared via melt infiltration in the temperature range between 90 and 450 °C.

To confirm the ordered tubular mesostructure of the OM-SiC-5 materials, we took the same three criteria as for the formation of tubular CMK-5 and discussed them in the following order:

• Increased or even higher relative intensity of the (110) reflection as compared to (100) in the low-angle X-ray diffraction patterns.

• Presence of the two pore types detected in the nitrogen physisorption measurements (pores between the tubes and in the tubes), where the same inner tube diameter should also be recognizable in the SBA-15/SiC composite material.

• TEM evidence for the hexagonal tubular structure.

Low-Angle XRD. Low-angle X-ray diffraction patterns of the OM-SiC-5 samples show significant differences as compared to OM-SiC-3 materials. In all cases, the relative intensity of the (100) reflection decreases, whereas the (110) reflection significantly increases (Figure 3). However, the composites samples (SiC/SBA-15) before HF treatment showed only one reflection (100) (in the same position of the corresponding OM-SiC-5 (100) reflection) without the presence of any others. The increase in the (110) and (200) intensities to the levels similar or even higher than the (100) intensity is observed only when a tubular replica is formed.[10,57–60,69] However, the exact intensity ratio depends on the tube geometry and arrangement.[59] In the case of OM-SiC-5 materials, this may occur because of the different physical and chemical nature of SMP-10, which may tend to form pore wall coatings of silica template (Scheme 1B) instead of filling them completely like in OM-SiC-3 (Scheme 1A).

The only material that was prepared via infiltration of SMP-10 into SBA-15 in an air atmosphere (at 90 °C, SiC-5-130-90X) had lowest relative intensity of (110) peak among all OM-SiC-5 materials. However, the pattern is quite different as compared to that of OM-SiC-3, where typically only the (100) peak was observed (Figure 1). Heating in air of SiC-5-130-90X sample may have resulted in partial oxygen cross-linking of the SMP-10 precursor and prevented formation of the silica pore wall coating. If the same infiltration procedure was employed in an inert atmosphere (argon) at 250 °C, the resulting SiC-5-135-250 material had a higher-intensity (110) reflection as compared to (100) (Figure 3). Lower amount of SMP-10 precursor introduced into the pores (SiC-5-130-250A) even at higher temperatures (SiC-5-130-350) did not result in any significant differences in low-angle XRD as compared to the SiC-5-130-250 sample. However, the intensities of (100) and (110) reflections became equal. As in the case of nanorod OM-SiC-3-80D material, which was prepared with a lower amount of PCS per pore volume ($A = 0.75$, Table 1), for SiC-5-130-250A and SiC-5-130-350 prepared with $A = 0.76$, a smaller amount of material was recovered after HF treatment and filtration (53 wt % ceramic yield) than for materials with $A = 0.91$. This value was still much higher as compared to SiC-3-S08-80D, where ceramic yield was 15 wt % only for $A = 0.75$. A reason might be the interaction of silica with SMP-10 and PCS as well as different synthesis temperatures of both templates (80 and 130 °C) resulting in different micropore openings between mesopores.[66]

Melt infiltration of SMP-10 ($A = 0.91$) in argon/vacuum atmosphere (250−450 °C, sample SiC-5-135-VM) and subsequent pyrolysis in vacuum at 1000 °C resulted in further changes of the diffraction patterns. For this sample, the (110) reflection had the highest intensity and the (100) almost disappeared. This is very similar to the carbon tubular replica of SBA-15 named CMK-5.[10,56–60] If instead of melt infiltration, wet impregnation was used (SiC-5-135-VL), the intensity of the (100) peak became higher. Because both vacuum-treated materials were prepared using the SBA-15 hydrothermally treated at higher temperature (135 °C) and in materials were pyrolyzed at lower temperature, the position of the low-angle reflections is shifted toward the lower 2θ values. High-angle XRD revealed that all OM-SiC-5 samples

(67) Bandosz, T. J. *J. Colloid Interface Sci.* **1997**, *193*, 127.
(68) Parida, S. K.; Dash, S.; Patel, S.; Mishra, B. K. *Adv. Colloid Interface Sci.* **2006**, *121*, 77.
(69) Bazuła, P. A.; Lu, A. H.; Nitz, J. J.; Schüth, F. *Microporous Mesoporous Mater.* **2008**, *108*, 266.

are amorphous (see the Supporting Information, Figure S3); however, the FT-IR measurements shows the presence of the Si−C bonds at 830 cm^{-1}.[27,29]

Nitrogen Physisorption Measurements of OM-SiC-5. According to the nitrogen physisorption measurements at 77 K, OM-SiC-5 materials have high specific surface areas in the range between 648 and 926 $m^2\ g^{-1}$ (Table 2), which is higher than for the OM-SiC-3 samples prepared using the same silica template (SBA-15 prepared at 130 and 135 °C) (Table 1). The lowest specific surface area of 648 $m^2\ g^{-1}$ was obtained for the SiC-5-130-90X sample, which was infiltrated in air atmosphere. Furthermore, the specific surface area and the pore volume (0.52 $cm^3\ g^{-1}$) are similar to that of the analogue nanorod replica SiC-3-M08-130 prepared from the same template and using the same polycarbosilane amount ($A = 0.91$). The pore size distribution was narrow with the maximum at ~3 nm of pore diameter. Also no secondary large mesopores were observed. Unlike the nanorod SiC-3-M08-130 analogue, the SiC-5-130-90X material before HF treatment showed no residual mesoporosity and very low specific surface area (15 m^2g^{-1}). Together with the low-angle X-ray diffraction measurements (which show lowest relative (110)/(100) peak intensity ratio among the OM-SiC-5 samples), one can estimate that in this case only a partial tubular structure was formed with part of the tubes that are filled (because of the oxygen cross-linking), blocking the access to the empty inner spaces.

The second sample in the Table 2 (SiC-5−130−250), which differed from the previous one in the infiltration temperature and atmosphere (250 °C and argon), had significantly higher specific surface area and pore volume (800 $m^2\ g^{-1}$ and 0.68 $cm^3\ g^{-1}$, respectively). The pore size distribution had a maximum at 3 nm and a shoulder in larger pore diameters (between 4 and 5 nm). However, for the primary composite of this materials with silica (before HF treatment) no porosity was measured that could fit the shoulder pores with larger diameter (Figure 4B). The original presence of the larger pores in the composite of the CMK-5 materials is typically considered as a proof for the presence of the tubular structure of this materials.[56] However, the CMK-5 materials are prepared in temperatures <1000 °C where the silica matrix remains stable.[10,58] It is known that at 1300 °C (which is the pyrolysis temperature of SiC-5−130−250), the SBA-15 sinters rapidly forming a dense material with surface areas below 1 m^2g^{-1},[31] but the presence of high-temperature stable silicon carbide inside the pores can hinder this process.[28] Two explanations of this observation are possible. One is that during the pyrolysis of the SiC-5-130-250 sample (before HF treatment) at 1300 °C, some of the SiO_2 from matrix or SiO (which can be formed because of the reaction between SiC and SiO_2) condense inside the formed nanotubes and close them until the HF treatment is made. The second explanation is that the shoulder with pore sizes between 4 and 5 nm represents a defect structure (like in case of OM-SiC-3). In our opinion, the first possibility, that the pores became blocked until HF treatment, seems more reasonable because X-ray diffraction patterns clearly indicate the possibility of tubular

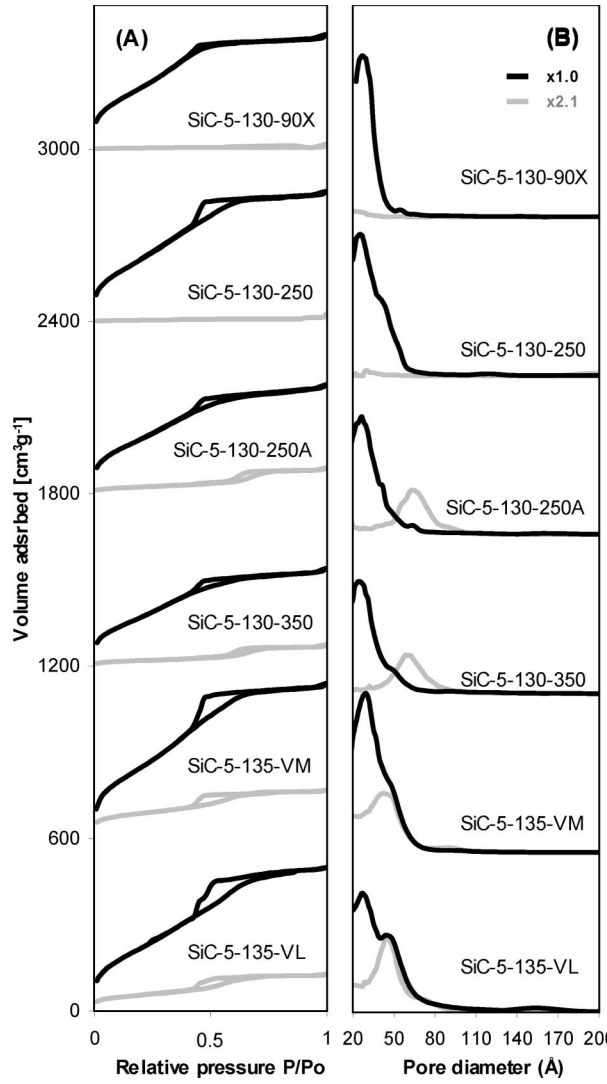

Figure 4. (A) Nitrogen physisorption isotherms (offset 0, 600, 1200, 1800, 2400, 3000 for each following sample from the bottom) and (B) BJH pore size distributions (calculated from adsorption branch of isotherm) of OM-SiC-5 materials prepared at 1300 °C in argon or at 1000 °C in a vacuum (-VM and -VL samples). Black lines indicate OM-SiC-5 materials, whereas gray lines represent their SBA-15/SiC composites (before HF treatment).

structure formation (Figure 3); also, the secondary large pores of defect structures of OM-SiC-3 materials had typically larger pore diameters in the range between 5 and 15 nm (Figure 2). Moreover, the specific surface area is significantly higher than for the OM-SiC-3 materials prepared using the same template.

Reducing the amount of precursor which was infiltrated into the pores from $A = 0.91$ to 0.76 (sample SiC-5-130-250A) resulted in the formation of porosity between 6 and 9 nm in diameter for composite materials (Figure 4). This pore size distribution does not correspond to the shoulder (4−5nm) which can be observed for OM-SiC-5-130-250A. An increase in the infiltration temperature to 350 °C (SiC-5-130-350) also did not result in the formation of pores in the composite materials that would correspond to a diameter of 4−5 nm. For both samples that were prepared with a lower amount of SMP-10 (SiC-5-130-250A and SiC-5-130-350), lower surface areas were measured (710 and 639 $m^2\ g^{-1}$, respectively). It could be attributed to the slightly lower amount of sample which was recovered after filtration (70

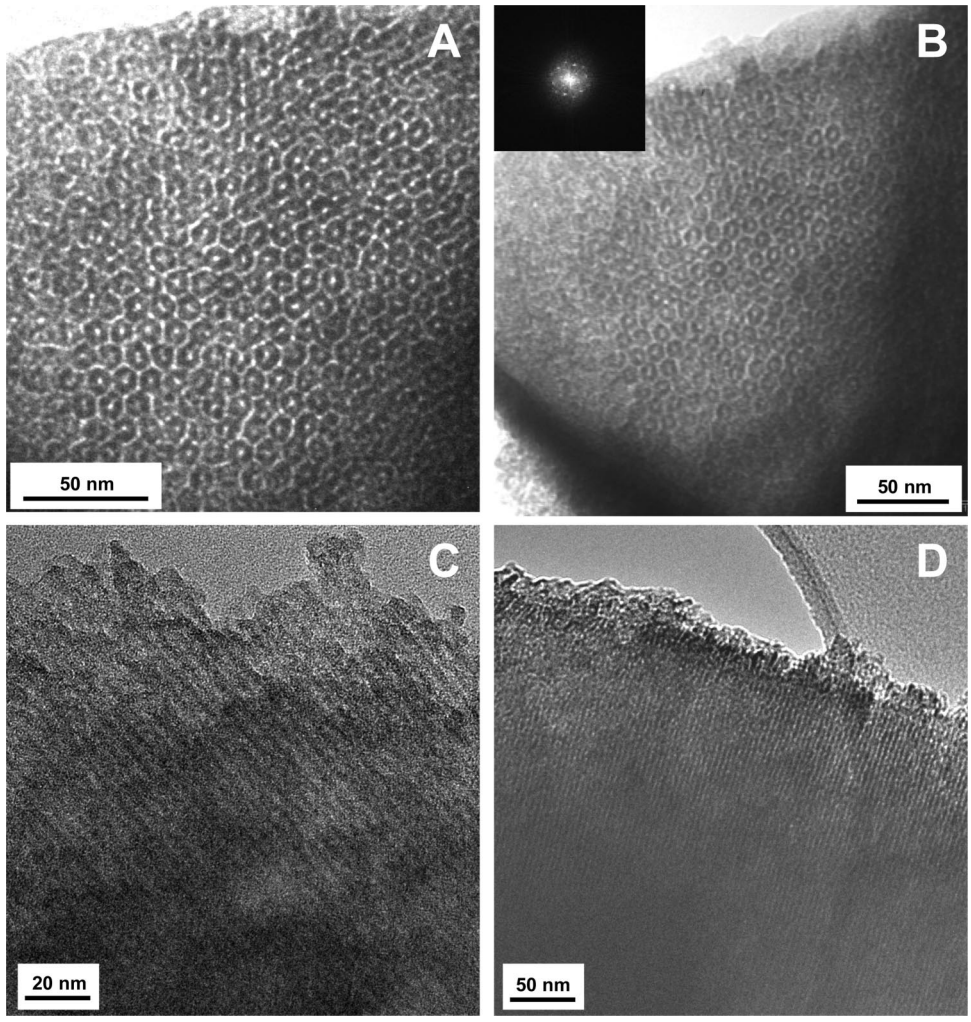

Figure 5. Transmission electron micrographs of the SiC-5−135-VM sample: (A, B) along the pore axis, (C, D) perpendicular to the pore axis. The inset in B represents its FFT image.

wt % typical recovery filtration of OM-SiC-5 prepared with $A = 0.91$), and the smallest particles/tubes/rods could have passed the filter.

By changing the SBA-15 template (to one treated at 135 °C, 1 nm in diameter larger pores as compared to 130 °C), applying a vacuum and pyrolysis at 1000 °C, it was possible to obtain ordered mesoporous silicon carbide with the tubular structure, where the pore size distribution of composite materials could be exactly fitted to the shoulder on the OM-SiC-5 pore size distribution (corresponding to the inner tube diameter P2, Scheme 1) (Figure 4, SiC-5-135-VM and SiC-5-135-VL samples). In addition to this, the measured specific surface areas were significantly higher as compared to other materials (Table 2). The SiC-5-135-VM sample prepared by SMP-10 infiltration without the organic solvents, had a specific surface area of 926 $m^2\ g^{-1}$ and pore volume of 0.82 $cm^3\ g^{-1}$, whereas for material where the SMP-10 was introduced as a solution (SiC-5-135-VL) these values were 840 $m^2\ g^{-1}$ and 0.76 $cm^3\ g^{-1}$, respectively. The ordered tubular structure of SiC-5-135-VM sample is also clearly visible on the transmission electron micrographs (Figure 5), both along the pore axis (A, B) and perpendicular to it (C, D).

Conclusions on the Preparation of the OM-SiC-5 Materials. Tubular ordered mesoporous silicon carbide with hexagonal mesostructure (OM-SiC-5) was prepared via nanocasting of SBA-15 silica with liquid vinyl-functionalized SMP-10 polycarbosilane precursor. Pyrolysis in a vacuum at 1000 °C was preferential and resulted in well-ordered materials with low-angle X-ray diffractograms and pore size distributions confirming the tubular structure. Moreover, for vacuum-pyrolyzed samples, the inner tube porosity was clearly visible before and after silica removal. This was not the case for materials that were pyrolyzed in argon at 1300 °C, but low-angle X-ray diffractograms as well as nitrogen sorption measurements after silica removal suggested also the tubular structure formation. No secondary large mesopores 5−15 nm in diameter were present (as in the case of some OM-SiC-3 materials), and very high specific surface areas (up to 926 $m^2\ g^{-1}$) were measured. The formation of tubular structure can be attributed to the silica−vinyl group interactions (π-bond of vinyl group with silica surface) leading to pore wall coating.[67,68] In addition, vacuum treatment is beneficial for preventing capillary condensation within the pores and avoiding complete filling of the silica pores and inner-tube pore blocking.

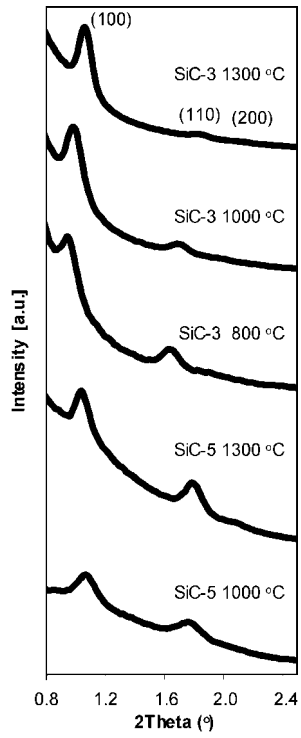

Figure 6. Low-angle X-ray diffraction patterns of the OM-SiC-3 and OM-SiC-5 samples pyrolyzed at various temperatures in argon.

3.3. Influence of Pyrolysis Temperature on the Properties, Chemical Composition, and Crystallinity of Ordered Mesorporous Silicon Carbide Materials with Hexagonal Pore Arrangement. Three OM-SiC-3 samples were prepared at 1300, 1000 and 800 °C and two OM-SiC-5 materials at 1300 and 1000 °C. All materials were pyrolyzed in argon and analyzed via the low- and high-angle XRD (Figure 6 and the Supporting Information, Figure S3), nitrogen physisorption (Figure 7), elemental analysis, and FT-IR (see the Supporting Information, Figure S4). The preparation condition as well as analysis data are summarized in Table 3.

Influence of Pyrolysis Temperature on OM-SiC-3. A batch of SiC-3-S14-135 (see Table 1 for details) was prepared, divided, and pyrolyzed in various temperatures (Table 3, named as SiC-3). According to high-angle X-ray diffractograms (see the Supporting Information, Figure S3), only the pyrolysis temperature of 1300 °C resulted in samples that showed reflections of the cubic, nanocrystalline β-SiC phase. This is in agreement with previous reports, where polymer nanocasting was used for the OM-SiC preparation and the presence of nanocrystalline β-SiC was detected for the pyrolysis temperatures above 1200 °C.[27,29] Extensive HR-TEM measurements were performed on OM-SiC-3 prepared at temperatures 1300 and 1400 °C (from templates hytrothermally treated at 100 and 130 °C) and selected area electron diffraction patterns (SAED) confirmed that the walls were composed of randomly oriented nanocrystalline β-SiC phase.[27,29] All materials prepared at 1000 and 800 °C were amorphous and no reflections were observed in wide-angle range. The decreased crystallinity with low pyrolysis temperatures was also observed by Shi et al.[29] The specific surface was increasing with the decreasing temperature of pyrolysis (Table 3).[29] We have also found that the OM-SiC-3 materials are slowly oxidized when exposed to air. Within 1 year after the synthesis, the wide-angle SiC reflections disappear, whereas the bulk, nonporous SiC retains its nanocrystalline structure in the same conditions.

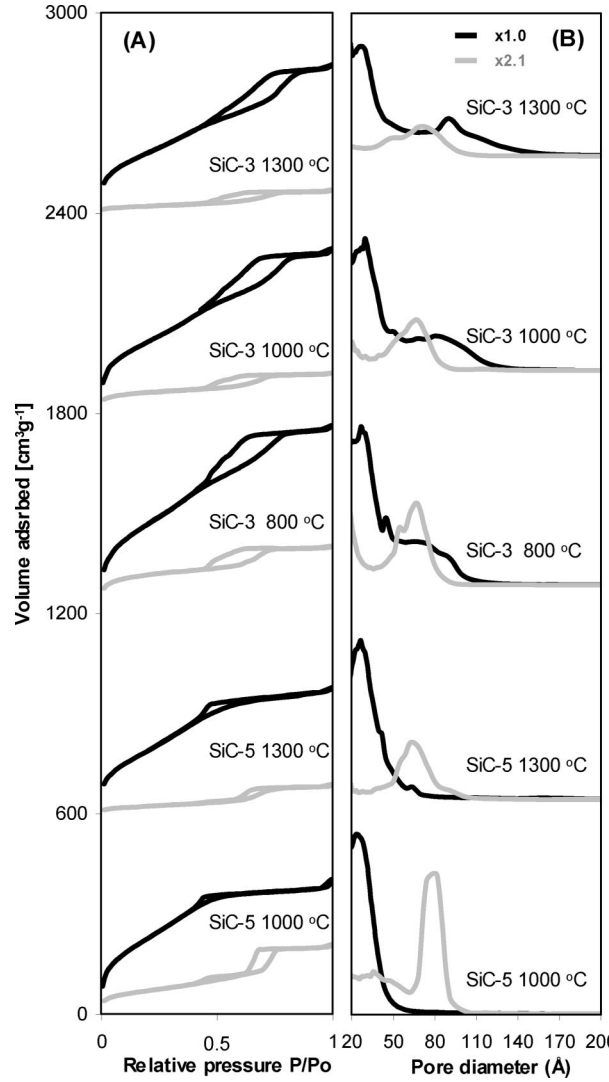

Figure 7. (A) Nitrogen physisorption isotherms (offset 0, 600, 1200, 1800, 2400 for each following sample from the bottom) and (B) BJH pore size distributions (calculated form adsorption branch of isotherm) of OM-SiC-3 and OM-SiC-5 materials prepared at various temperatures in argon. Black lines indicate OM-SiC-3 or OM-SiC-5 materials, whereas gray lines represent their SBA-15/SiC composites (before HF treatment).

Table 3. Heat Treatment and Analysis Data of OM-SiC-3 and OM-SiC-5 Prepared by Pyrolysis in Argon Atmosphere at Different Temperatures

sample code[a]	T_p[b]	C (wt %)	O (wt %)	H (wt %)	S_g^{comp} (m^2g^{-1})[b]	S_g^{SiC} (m^2g^{-1})
SiC-3	1300	29.3	13.1	1.2	77	672
	1000	31.2	16.6	2.1	222	792
	800	29.1	12.5	2.6	411	991
SiC-5	1300	28.9	18.3	1.8	86	710
	1000	28.5	18.0	2.2	255	854

[a] See Tables 1 and 2 for sample details (SiC-3 is SiC-3-S14-135, whereas SiC-5 is SiC-5-130-250). [b] T_p = pyrolysis temperature. [c] Specific surface area of SiC/SBA-15 composite before HF treatment.

The crystallite size calculated according to the Scherrer equation was similar for all crystalline OM-SiC-3 samples (pyrolyzed at 1300 °C) and was ~1.7 nm (± 0.2 nm). Materials prepared from larger pore templates showed higher peak intensities; however, the crystallite size was smilar (even

for the "bulk SiC" prepared without template. This could be due to the increased amount of oxycarbide species of high surface area materials.

The FT-IR measurements confirmed SiC formation and Si−C bonds were detected at ~830 cm^{-1} (see the Supporting Information, Figure S4) for all samples as most intensive peak. As expected, in addition to the Si−C bonds, Si−O vibrations were present at ~1056 cm^{-1}; this is due to the presence of silicon oxycarbides on the surface of silicon carbide. The silicon oxycarbides are known to be formed on high-surface-area silicon carbide due to the oxidation in air at ambient conditions or at the SiC/SiO_2 boundary at higher temperatures.[70–72] If the specific surface area of silicon carbide (or SiC/SiO_2 boundary) is high, then one also expects the high amounts of silicon oxycarbides in the sample. Silicon oxycarbide may also be effect of silicon carbide oxidation at high temperatures by oxygen residues from argon gas used in the pyrolysis.

The relative intensity of the Si−O to SiC peak was lowest for sample prepared at 1300 °C, suggesting the lowest oxygen content.[28,31] However, if the pyrolysis temperature was decreased, the intensity of the Si−O peak increased. This shows that the amount of oxygen was higher and could be mainly attributed to the higher specific surface area and larger SiC/SiO_2 interface. This observation is in the agreement with the elemental analysis data (Table 3), which showed that the amount of oxygen increases from 13.1 to 16.6 wt % for samples calcined at 1300 and 1000 °C, respectively. Shi et al. reported also high oxygen content of 14 wt % in ordered mesoporous silicon carbide (surface area of 540 $m^2\ g^{-1}$ pyrolysis temperature 1400 °C).[29] The IR spectra that was presented in the same report showed increasing intensity of the Si−O peak with lowering of the pyrolysis temperature and was in agreement with data presented here. The XPS measurement of mesoporous silicon carbide materials (with 260 $m^2\ g^{-1}$, pyrolyzed at 1000 °C) performed by Yan et al. and subsequent analysis of Si 2p peak revealed that 18 at. % Si is in the form of SiO_xC_y.[25]

Further reduction of the pyrolysis temperature to 800 °C resulted in increased specific surface area (991 $m^2\ g^{-1}$) and lowest oxygen level among OM-SiC-3 materials, 12.5 wt %. This can be attributed to decreased formation of SiO_xC_y at the SiC/SiO_2 boundary at lower temperatures and different chemical nature of the polymer-derived SiC materials treated at such low temperatures (high H content of 2.6 wt % also suggests lower degree of the SiC densification due to the incomplete removal of methane groups). The presence of oxycarbide species lowers also the relative concentration of Si in these materials and therefore the Si content is in the range between 50 and 56 wt %, which is lower than for the pure SiC (70 wt % Si)

However, further investigations and analytical techniques (XPS, NMR) are required for the more exact determination of oxygen origin in OM-SiC materials, which is beyond the scope of this report.[28,31]

Sorption data indicated slight changes in the pore sizes and pore volumes resulting from lower shrinkage at lower pyrolysis temperatures, but the overall pore structure remained (Figure 7). The lower shrinkage of materials pyrolyzed at low temperatures was also observed on low angle X-ray diffraction patterns (Figure 6). The position of (100) reflection was located at $2\theta = 1.06$ for materials prepared at 1300 °C, whereas for a pyrolysis at 800 °C, this reflection was at $2\theta = 0.96$. Interestingly, the lower synthesis temperatures also resulted in slightly more intense (110) reflection. The total amount of carbon did not change significantly for each sample. The highest value was observed for a sample prepared at 1000 °C (31.2 wt %, Table 3), whereas materials prepared at 800 °C had 29.1 wt % carbon. These values are close to the carbon content of pure and stoichmiometric SiC (30 wt %). On the one hand, presence of the silicon oxycarbides should also lower the carbon content of materials, but on the other hand, pyrolysis of preceramic polymer is known to yield SiC ceramics with excessive free carbon.

Influence of Pyrolysis Temperature on OM-SiC-5. Two OM-SiC-5 materials were prepared (SiC-5, Table 3) using similar procedures as for SiC-5-130-250 (Table 3; only the pyrolysis temperature changed). Pyrolysis was performed in argon at 1300 and 1000 °C. Similar observations to SiC-3 materials where made and the specific surface area was increasing with lowering of the pyrolysis temperature. As in the case of composite materials, a significant increase in the specific surface area was observed (from 86 to 255 $m^2\ g^{-1}$) when the temperature was decreased. These values are higher as for the corresponding SiC-3 samples prepared at the same temperatures. According to the wide-angle X-ray diffraction patterns, all SiC-5 materials were amorphous (see the Supporting Information, Figure S3).

Interestingly, in case of the SiC-5 composite sample (before silica removal) prepared at 1000 °C, a bimodal pore size distribution is observed (Figure 7). One pore system that corresponds to the incomplete silica pore filling with PCS (because materials were prepared with A = 0.76) can be observed in the range of 7−9 nm (also for material prepared at 1300 °C, but slightly shifted toward lower pore volume). The second pore system appears to be located between 3 and 5 nm and does not appear in materials prepared at 1300 °C. This value corresponds well to the inner diameter of the tubes of the OM-SiC-5 materials and shows that lower temperatures of pyrolysis can avoid blocking of the tubular structures in the composite materials. Additionally, low-angle X-ray diffraction patterns (Figure 6) show no significant changes in the structure and (100)/(110) peak intensity ratio remains constant.

The elemental analysis shows generally higher oxygen content (18.0−18.3 wt %) in SiC-5 materials as compared to SiC-3 samples. This can be due to the higher specific surface area of tubular materials or differences in chemical properties which result from using different precursor (SMP-10). However, significant difference in oxygen concentration was observed as compared to the sample discussed above which was prepared in vacuum (SiC-5-135-VM, Table 2). The SiC-5-135-VM materials showed only 9.7 wt % oxygen

(70) Merlemejean, T.; Abdelmounim, E.; Quintard, P. *J. Mol. Struct.* **1995**, *349*, 105.
(71) Onneby, C.; Pantano, C. G. *J. Vac. Sci. Technol., A* **1997**, *15*, 1597.
(72) Radtke, C.; Baumvol, I. J. R.; Morais, J.; Stedile, F. C. *Appl. Phys. Lett.* **2001**, *78*, 3601.

Scheme 2. Schematic Explanation for *Ia3d* Symmetry Transformations of OM-SiC-8 Materials Due to the Changing Connectivity between Two Independent Mesopore Networks of KIT-6 Template: (A) Connected, (B) Isolated

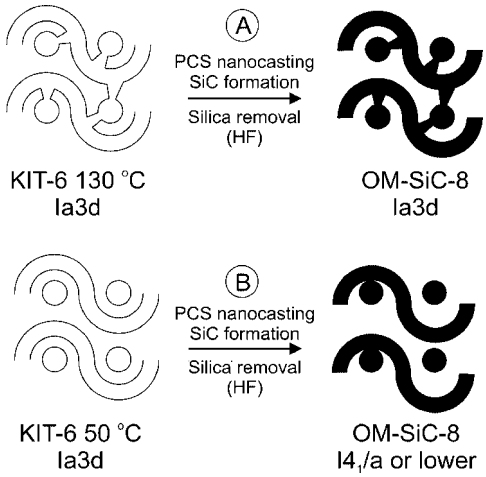

content, and a similar value could also be detected for the other OM-SiC-5 materials, which were prepared in vacuum at 1000 °C. This means that the vacuum treatment is not only beneficial for the preparation of high-surface-area tubular structures but also for lowering the oxygen amount in them. The FT-IR measurements of SiC-5 samples were similar to the SiC-3 and higher relative intensity of the Si−O peak was measured for the material prepared at low temperature (see the Supporting Information, Figure S4).

Conclusions on the Influence of Pyrolysis Temperature on OM-SiC-3 and OM-SiC-5 Materials. The pyrolysis temperature of OM-SiC-3 and OM-SiC-5 materials in argon atmosphere had a significant influence on their specific surface areas and elemental composition. When treated at 1300 °C, OM-SiC-3 was nanocrystalline showing the presence of cubic β-SiC, whereas OM-SiC-5 was amorphous. For lower temperatures, no crystalline phase was detected. Lower temperature resulted in higher specific surface areas measured and significantly influenced the oxygen content. If instead of argon treatment OM-SiC-5 materials were pyrolyzed under vacuum, the oxygen content (present in form of silicon oxycarbides) could significantly be decreased (by almost 50%).

3.4. Symmetry Changes of Cubic Ordered Mesoporous Silicon Carbide (OM-SiC-8), Induced Using the KIT-6 Template with Different Pore Connectivity. As already shown by Shi et al.,[29] the cubic ordered mesoporous silica KIT-6 can be used as a hard template for the preparation of ordered mesoporous silicon carbide with cubic pore arrangement. However, the KIT-6 templates were hydrothermally treated at high temperatures (100 and 130 °C), resulting in OM-SiC-8 materials having the same (Ia3d) symmetry as the host silica (Scheme 2A). This is due to the micropore connectivity between two independent mesopore channels of KIT-6 formed during the hydrothermal treatment above 80 °C.[73] Here, we also observed that it is also possible to obtain cubic silicon carbide with lower symmetry ($I4_1/a$ or lower) if the KIT-6 matrix treated at 50 °C is used as template (Scheme 2B). Low hydrothermal treatment of KIT-6 (50 °C) results in two independent pore systems that are not connected (Scheme 2B) and therefore a displacement between the nanorods formed inside them takes place after silica removal resulting in lower symmetry. This effect was already extensively studied for the carbon and metal replica of another cubic Ia3d ordered mesoporous silica (MCM-48)[6,74] and also reported for a replica of KIT-6.[19,73,75]

Here, we used melt impregnation of low molecular weight PCS (M_w = 800) at 320 °C of KIT-6 templates prepared at 130, 100, and 50 °C (Table 4). According to low-angle X-ray diffraction patterns (Figure 8), in the case of 130 and 100 °C templates, an inverse ordered mesoporous silicon carbide replica was obtained, where (211) and (200) reflections could be identified (at 2θ = 1.08 and 1.26, respectively). When the KIT-6 prepared at 50 °C was used as template, the (211) reflection was shifted toward higher 2θ values (template with smaller unit cell was used) and additional very intense peak was detected at ~0.73 2θ. It was several times indicated in the literature, that the appearance of this reflection is attributed to the synthesis of lower-symmetry inverse replicas (CMK-1-like) of the *Ia3d* mesoporous materials like MCM-48 or KIT-6.[6,74] Extensive studies and simulations of this effect in carbon materials were performed via HRTEM and electron crystallography by Kaneda et al.[76] Our preliminary TEM investigations of the SiC-5-50 sample showed that the

Table 4. OM-SiC-8 Prepared at 1300 °C from Aldrich PCS with M_w = 800 (melt infiltration at 320 °C)[a]

sample code[b]	T_{SBA-15} (°C)	A (g/cm^3)	S_g^{comp} (m^2g^{-1})	V_p (cm^3g^{-1})	S_g^{SiC} (m^2g^{-1})
SiC-8-130	130	0.91	94	0.74	807
SiC-8-100	100	0.91	90	0.57	648
SiC-8-50	50	0.95	7	0.32	418

[a] Abbreviations are the same as those in previous tables. [b] Sample codes are SiC-8-YYY, where YYY is temperature of silica hydrothermal treatment in °C.

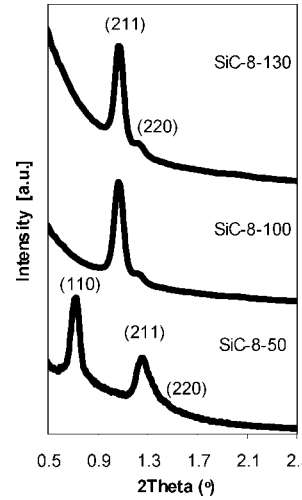

Figure 8. Low-angle X-ray diffraction patterns of the OM-SiC-8 materials.

(73) Kim, T. W.; Kleitz, F.; Paul, B.; Ryoo, R. *J. Am. Chem. Soc.* **2005**, *127*, 7601.
(74) Yang, C. M.; Sheu, H. S.; Chao, K. J. *Adv. Funct. Mater.* **2002**, *12*, 143.
(75) Kim, T. W.; Solovyov, L. A. *J. Mater. Chem.* **2006**, *16*, 1445.
(76) Kaneda, M.; Tsubakiyama, T.; Carlsson, A.; Sakamoto, Y.; Ohsuna, T.; Terasaki, O. *J. Phys. Chem. B* **2002**, *106*, 1256.

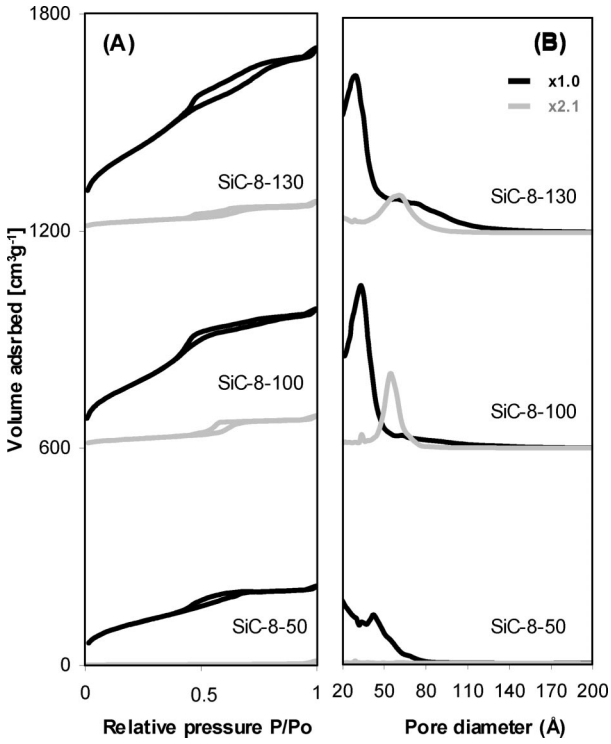

Figure 9. (A) Nitrogen physisorption isotherms (offset 0,600,1200) and (B) BJH pore size distributions (adsorption) of OM-SiC-8 materials. Black lines indicate OM-SiC-5 materials, whereas gray lines represent their SBA-15/SiC composites (before HF treatment).

mesostructure lattice planes can be detected with the distance corresponding to that of the (110) and (211) low angle XRD reflection (12.3 and 7.1 nm, respectively, see the Supporting Information, Figure S5). The (110) lattice plane was neither observed for the KIT-6 nor for the SiC-8−100 or SiC-8−130 sample.

The nitrogen physisorption measurements showed that high-surface-area OM-SiC-8 materials were obtained (between 418 and 807 $m^2\ g^{-1}$) with type IV adsorption isotherms (Figure 9A). Similar amounts of PCS per mesopore volume were used for each sample, and the highest surface area was measured for SiC-8-130 prepared from large pore 130 °C template. The pore size distribution of this sample shows the maximum at around 2.9 nm (pores between nanorods) and secondary mesoporosity between 5 and 10 nm, which can be attributed to poorly ordered nanorod structures (similar to OM-SiC-3 materials with defects) (Figure 9B). This defect structure also causes high mesopore volumes to be measured (0.74 $cm^3\ g^{-1}$).

When the KIT-6 template prepared at 100 °C was used, lower specific surface area and mesopore volumes for the SiC-8−100 were obtained (648 $m^2\ g^{-1}$ and 0.57 $cm^3\ g^{-1}$). Additionally no secondary mesoporosity was present and the maximum of pore size distribution was shifted toward higher values (3.3 nm in diameter).

In the case of SiC-8-50 material, where a decrease in symmetry was observed, low specific surface area and pore volumes were measured (418 $m^2\ g^{-1}$ and 0.32 $cm^3\ g^{-1}$) and the pore diameter shifted to even higher values (4.4 nm maximum was observed on the BJH graph). The low surface area may be a result of too high amount of the PCS precursor used and should be a subject of optimization (together with the infiltration conditions). Kim et al. showed that the preparation methods of CMK-8 materials from low-temperature-treated KIT-6 materials have significant influence on the final carbon properties.

4. Conclusions

In this paper, for the first time, we have shown how to prepare hexagonally ordered tubular mesoporous carbide (OM-SiC-5) and investigated the influence of the preparation conditions on its structure. Moreover, we demonstrated that the symmetry lowering can be obtained for cubic OM-SiC-8 materials if ordered mesoporous silica (KIT-6) hydrothermally treated at low temperature is used. We have shown that the molecular weight of PCS precursors have significant influence on the properties of nanorod OM-SiC-3 inverse replica of SBA-15. Too high molecular weights of PCS can cause the formation of defects and disordered structures with bimodal pore size distributions. However, no significant changes were observed if melt impregnation or wet infiltration with solvent was used. The materials prepared had specific surface areas between 418 and 991 $m^2\ g^{-1}$, which were strongly dependent not only on the pore size of the template silica but also on the PCS pyrolysis temperature (lower temperatures resulted in materials with higher surface areas). For the formation of tubular OM-SiC-5 structures, pyrolysis in a vacuum at 1000 °C was found to give the best results with very high surface areas and low oxygen content (9.7 wt.%).

Acknowledgment. Piotr Krawiec thanks Prof. Avelino Corma for helpful discussions and financial support.

Supporting Information Available: Additional figures and tables (PDF). This material is available free of charge via the Internet at http://pubs.acs.org.

CM801035G